DALTON

Mono- and bi-nuclear titanium imido complexes supported by aryloxide ligands: fine control by *ortho* substituents‡

Philip E. Collier, Alexander J. Blake and Philip Mountford*†

Department of Chemistry, University of Nottingham, Nottingham, UK NG7 2RD

Reaction of the titanium imido complexes $[Ti(NR)Cl_2(py)_3]$ (R = Bu^t, $C_6H_3Me_2$-2,6 or $C_6H_3Pr^i_2$-2,6; py = pyridine) with 2 equivalents of lithium aryloxide $Li[OC_6H_3R'_2$-2,6] (R′ = Me, Pr^i or Bu^t) afforded the mononuclear four- or five-co-ordinate or binuclear four-co-ordinate complexes $[\{Ti(NR)(OC_6H_3R'_2$-2,6$)_2(py)_n\}_m]$ (m = 1, n = 1 or 2; m = 2, n = 0) depending on the identity of R and R′. The crystal structures of $[Ti_2(\mu$-$NBu^t)_2(OC_6H_3Me_2$-2,6$)_4]$ **1** and $[Ti(NC_6H_3Me_2$-2,6$)(OC_6H_3Me_2$-2,6$)_2(py)_2]$ have been determined. Extended-Hückel molecular orbital calculations for models of **1** showed that the deviation of the μ-imido Bu^t substituents from coplanarity with the Ti_2N_2 core in this and some related species can be attributed to a second-order Jahn–Teller distortion.

The synthesis, structures, bonding and reactivity of transition-metal imido complexes continue to attract considerable interest.[1–3] Terminal titanium imido complexes were first structurally characterised in 1990,[4,5] and since then a number of simple mononuclear, five- and six-co-ordinate titanium imido derivatives have been reported. Many of these have recently been reviewed by Wigley.[3] We recently described[6,7] the readily available synthons $[Ti(NR)Cl_2L_n]$ [R = Bu^t or aryl; L = pyridine (py) or $NC_5H_4Bu^t$-4; n = 2 or 3] from which a range of new classes of titanium imido derivative may be prepared.[8–13] Examples of mononuclear, five-co-ordinate, aryloxide-supported Group 4 imido derivatives have been prepared previously by Rothwell and co-workers.[14] However, the dependence of the structures, nuclearity and metal co-ordination number of the imido complex upon the imide and alkoxide ligand substituents has not previously been systematically probed in these systems. An understanding of these controlling factors is essential for complex design and preparation. Here we report reactions of $[Ti(NR)Cl_2(py)_3]$ (R = Bu^t, $C_6H_3Me_2$-2,6 or $C_6H_3Pr^i_2$-2,6) with lithium aryloxides to form mono- or bi-nuclear titanium imido bis(aryloxide) derivatives whose structures depend critically on the identity of the *ortho* substituents of the aryloxide ligands. We also describe a group theoretical analysis and extended-Hückel molecular orbital calculations that probe the electronic structure and molecular geometry of $[Ti_2(\mu$-$NBu^t)_2(OC_6H_3Me_2$-2,6$)_4]$ and some related binuclear μ-imido complexes.§

Results

Synthesis and characterisation of the new complexes

The titanium imido dichloride complexes $[Ti(NR)Cl_2(py)_3]$ (R = Bu^t, $C_6H_3Me_2$-2,6 or $CH_6H_3Pr^i_2$-2,6) were prepared according to previously described procedures.[7] Previous studies in our group have shown that new titanium imido derivatives may be readily obtained from these precursors by straightforward metathesis reactions. Our approach to new aryloxide-supported titanium imido complexes was therefore along similar lines. The new compounds reported in this contribution are shown in Schemes 1 and 2. We shall first consider the *tert*-butyl imido complexes (Scheme 1).

Reaction of $[Ti(NBu^t)Cl_2(py)_3]$ with 2 equivalents of Li[OPh] in thf at −25 °C failed to produce any tractable product. However, use of the *ortho*-dimethylated analogue $Li[OC_6H_3Me_2$-2,6] under identical conditions afforded the dark red, binuclear complex $[Ti_2(\mu$-$NBu^t)_2(OC_6H_3Me_2$-2,6$)_4]$ **1** in 37% isolated yield after crystallisation from pentane. The crystals of **1** were suitable for X-ray diffraction analysis. The molecular structure is shown in Fig. 1, selected bond lengths and angles are listed in Table 1. The solution ^{1}H and ^{13}C-{^{1}H} NMR data for **1** are consistent with the solid-state structure.

Table 1 Selected bond lengths (Å) and angles (°) for $[Ti_2(\mu$-$NBu^t)_2(OC_6H_3Me_2$-2,6$)_4]$ **1**. Atoms carrying the suffix B are related to their counterparts by the symmetry operator $-x + 2, -y, -z$

Ti(1)···Ti(1B)	2.7909(7)	Ti(1)–O(2)	1.811(1)
Ti(1)–N(1)	1.885(2)	N(1)–C(1)	1.478(3)
Ti(1)–N(1B)	1.924(2)	O(1)–C(11)	1.346(2)
Ti(1)–O(1)	1.811(1)	O(2)–C(21)	1.347(2)
Ti(1B)···Ti(1)–N(1)	43.44(5)	N(1B)–Ti(1)–O(2)	119.14(7)
Ti(1B)···Ti(1)–N(1B)	42.33(5)	O(1)–Ti(1)–O(2)	109.71(7)
N(1)–Ti(1)–N(1B)	85.78(7)	Ti(1)–N(1)–Ti(1B)	94.22(7)
Ti(1B)···Ti(1)–O(1)	124.08(5)	Ti(1)–N(1)–C(1)	136.6(1)
N(1)–Ti(1)–O(1)	117.53(7)	Ti(1B)–N(1)–C(1)	126.5(1)
N(1B)–Ti(1)–O(1)	111.10(7)	Ti(1)–O(1)–C(11)	168.3(1)
Ti(1B)···Ti(1)–O(2)	126.21(5)	Ti(1)–O(2)–C(21)	173.2(1)
N(1)–Ti(1)–O(2)	112.17(7)		

Molecules of $[Ti_2(\mu$-$NBu^t)_2(OC_6H_3Me_2$-2,6$)_4]$ **1** lie across crystallographic inversion centres and contain two four-co-ordinate titanium centres linked by the two μ-NBu^t ligands with the remainder of each metal co-ordination sphere comprising two terminal $OC_6H_3Me_2$-2,6 moieties. The aryloxide linkages are essentially linear [Ti(1)–O(1)–C(11) 168.3(1) and Ti(1)–O(2)–C(21) 173.2(1)°] and the co-ordination geometry at the μ-nitrogen atoms is nearly trigonal planar [sum of the angles subtended at N(1) = 357.3(2)°] with N(1) lying only 0.15 Å out of the computed Ti(1), Ti(1B), C(1) least-squares plane. Interestingly, however, the Bu^t substituents are somewhat bent out of the Ti_2N_2 planar core as evidenced by N(1B)···N(1)–C(1) 165.7(2)° which corresponds to a 0.33 Å displacement of C(1) from the Ti(1), Ti(1B), N(1), N(1B) least-squares plane. A search of the Cambridge Structural Database[16,17] showed that this is a common feature of many binuclear, Group 4 bis(μ-imido) complexes. We address in detail the electronic origins of this feature for **1** and for the related tetrakis(dimethylamido) analogue $[Ti_2(\mu$-$NBu^t)_2(NMe_2)_4]$[18,19] below.

When a $CDCl_3$ solution of $[Ti_2(\mu$-$NBu^t)_2(OC_6H_3Me_2$-2,6$)_4]$ **1** was treated with *ca*. 12 equivalents of pyridine new Bu^t and $OC_6H_3Me_2$-2,6 group signals (78% conversion) grew into the ^{1}H NMR spectrum over 4 d suggesting formation of a new species **2**. The same compound can be obtained from the reaction of

† E-Mail: philip.mountford@nottingham.ac.uk

‡ *Non-SI unit employed*: eV ≈ 1.60 = 10^{-19} J.

§ Although for ease of representation all titanium–imido linkages are drawn 'Ti=NR', the formal metal–ligand multiple bond order in the complexes described herein is probably best thought of as three (pseudo-σ^2 π^4, triple bond) rather than as two.[3]

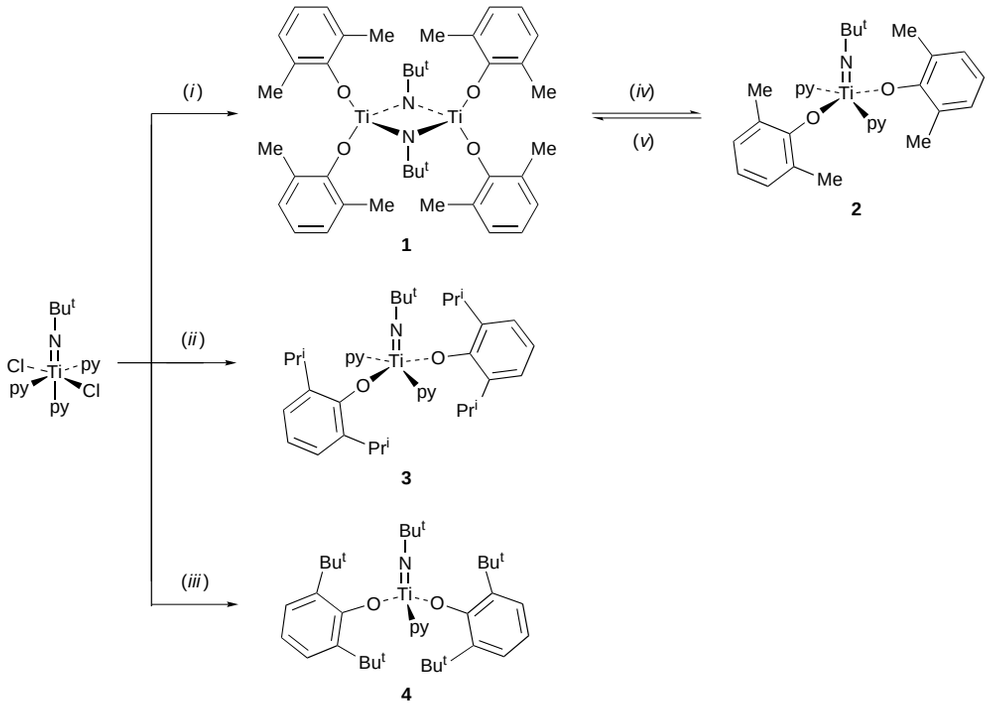

Scheme 1 Reagents and conditions: (*i*) Li[$OC_6H_3Me_2$-2,6] (2 equivalents), tetrahydrofuran (thf), −25 °C then room temperature (r.t.), 18 h, yield 37%; (*ii*) Li[$OC_6H_3Pr^i_2$-2,6] (2 equivalents), thf, −40 °C then r.t., 15 h, 59%; (*iii*) Li[$OC_6H_3Bu^t_2$-2,6] (2 equivalents), thf, −50 °C then r.t., 16 h, 81%; (*iv*) py (12 equivalents), $CDCl_3$, r.t., 4 d, *ca.* 80%; (*v*) $CDCl_3$, r.t., 6 d, *ca.* 70%

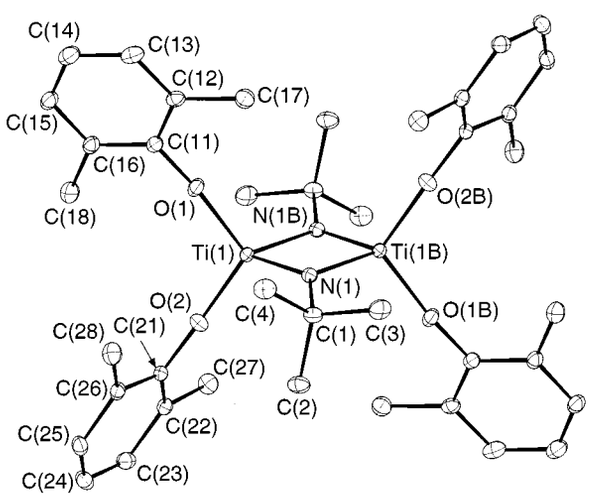

Fig. 1 A CAMERON[15] plot of [$Ti_2(\mu\text{-}NBu^t)_2(OC_6H_3Me_2$-2,6)$_4$] **1**. Hydrogen atoms are omitted for clarity and the thermal ellipsoids are drawn at the 20% probability level. Atoms carrying the suffix B are related to their counterparts by the symmetry operator $-x + 2, -y, -z$

[$Ti(NBu^t)Cl_2(py)_3$] with 2 equivalents of Li[$OC_6H_3Me_2$-2,6] in the presence of *ca.* twenty-fold excess of pyridine. The yellow compound **2** cannot be obtained free of additional pyridine and was only isolated as an oil. However, on the basis of the similarity of the ^{1}H and ^{13}C-{^{1}H} NMR spectra of **2** to those of other bis(pyridine) complexes we have fully characterised (see below) we propose that **2** is the mononuclear species [$Ti(NBu^t)(OC_6H_3Me_2$-2,6)$_2(py)_2$] as shown in Scheme 1. Compound **2** is unstable with respect to loss of pyridine and dimerisation in solution. Thus $CDCl_3$ solutions of **2** (contaminated with *ca.* 0.4 equivalent of free pyridine) slowly change colour at room temperature over *ca.* 6 d and the resulting ^{1}H NMR spectra show new resonances attributable to **1** (*ca.* 70% conversion).

Treatment of [$Ti(NBu^t)Cl_2(py)_3$] with 2 equivalents of lithiated bulkier aryloxides, namely Li[$OC_6H_3Pr^i_2$-2,6] and Li[$OC_6H_3Bu^t_2$-2,6] afforded the five- and four-co-ordinate mononuclear complexes [$Ti(NBu^t)(OC_6H_3Pr^i_2$-2,6)$_2(py)_2$] **3** (59%, yellow) and [$Ti(NBu^t)(OC_6H_3Bu^t_2$-2,6)$_2(py)$] **4** (81%, orange) respectively. The solution ^{1}H and ^{13}C-{^{1}H} NMR data for **3** are consistent with the structure shown in Scheme 1. We assume a near-trigonal bipyramidal titanium centre with mutually *trans* pyridine ligands occupying quasi-axial positions by analogy with the crystallographically characterised homologue [$Ti(NC_6H_3Me_2$-2,6)$(OC_6H_3Me_2$-2,6)$_2(py)_2$] **5** (see below).

We have not been able to isolate diffraction-quality crystals of [$Ti(NBu^t)(OC_6H_3Bu^t_2$-2,6)$_2(py)$] **4** but we formulate it as a monomeric, four-co-ordinate complex on the basis of solution molecular weight measurements in dichloromethane. The ^{1}H and ^{13}C-{^{1}H} NMR data and elemental analysis for **4** support the structure shown in Scheme 1.

In order to explore the importance of the imido nitrogen substituent in these systems we have also prepared the aryloxide-supported titanium arylimido complexes shown in Scheme 2. Thus treatment of [$Ti(NC_6H_3R_2$-2,6)$Cl_2(py)_3$] (R = Me or Pr^i) with 2 equivalents of Li[$OC_6H_3Me_2$-2,6] in thf gave the red-brown, monomeric, five-co-ordinate derivatives [$Ti(NC_6H_3R_2$-2,6)$(OC_6H_3Me_2$-2,6)$_2(py)_2$] (R = Me **5** or Pr^i **6**) in 62 and 36% yield, respectively. Unlike the 2,6-dimethylphenoxide-supported *tert*-butyl imido derivative **2** the complexes **5** and **6** show no apparent tendency to lose pyridine and dimerise.

Red diffraction-quality crystals of [$Ti(NC_6H_3Me_2$-2,6)-$(OC_6H_3Me_2$-2,6)$_2(py)_2$] **5** were obtained from a cold hexane solution. The molecular structure of **5** is shown in Fig. 2 and selected bond lengths and angles are listed in Table 2. Molecules of **5** lie across crystallographic two-fold rotation axes. The Ti–N(1)–C(15) linkage is constrained to linearity by crystal symmetry, the aryloxide linkages are approximately linear [Ti–O(1)–C(7) 162.7(2)°] and the Ti=N and Ti–O bond lengths lie within the ranges reported for related systems.[14,20] The geometry at titanium is approximately trigonal bipyramidal with the mutually *trans* pyridine ligands occupying the axial positions.

Reaction of [$Ti(NC_6H_3Pr^i_2$-2,6)$Cl_2(py)_3$] with 2 equivalents of the bulky Li[$OC_6H_3Bu^t_2$-2,6] afforded a yellow derivative which we formulate as the bis(pyridine) complex [$Ti(NC_6H_3$-

Table 2 Selected bond lengths (Å) and angles (°) for [Ti($NC_6H_3Me_2$-2,6)($OC_6H_3Me_2$-2,6)$_2$(py)$_2$] **5**. Atoms carrying the suffix B are related to their counterparts by the symmetry operator $-x, y, -z + \frac{1}{2}$

Ti(1)–N(1)	1.734(4)	Ti(1)–O(1)	1.884(2)
Ti(1)–N(2)	2.244(3)		
N(1)–Ti(1)–O(1)	113.96(8)	O(1)–Ti(1)–N(2)	87.02(10)
N(1)–Ti(1)–N(2)	99.33(8)	N(2B)–Ti(1)–N(2)	161.3(2)
O(1)–Ti(1)–O(1B)	132.1(2)	Ti(1)–N(1)–C(15)	180
O(1)–Ti(1)–N(2B)	85.43(10)	Ti(1)–O(1)–C(7)	162.7(2)

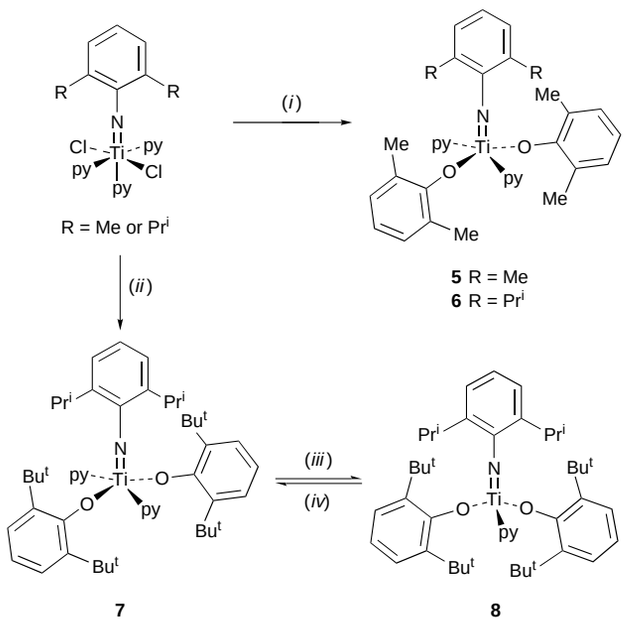

Scheme 2 Reagents and conditions: (*i*) for **5**, Li[$OC_6H_3Me_2$-2,6] (2 equivalents), thf, −50 °C then r.t., 15 h, 62%; for **6**, Li[$OC_6H_3Me_2$-2,6] (2 equivalents), thf, −50 °C then r.t., 14 h, 36%; (*ii*) Li[$OC_6H_3Bu^t_2$-2,6] (2 equivalents), thf, −50 °C then r.t., 16 h, 32%; (*iii*) in $CDCl_3$ solution at r.t.; (*iv*) in the solid state

Pr^i_2-2,6)($OC_6H_3Bu^t_2$-2,6)$_2$(py)$_2$] **7** in the solid state. In solution, however, this species appears to dissociate one of the pyridine ligands since ^{1}H and ^{13}C-{^{1}H} NMR spectra show signals attributable to $NC_6H_3Pr^i_2$-2,6 and $OC_6H_3Bu^t_2$-2,6 groups (1 : 2 by ^{1}H NMR spectroscopy) and also to two pyridine ligand environments (1 : 1 ratio), the signals for one of which are exactly coincident with those of free pyridine. Thus **7** probably gives rise to the mono(pyridine) adduct [Ti($NC_6H_3Pr^i_2$-2,6)($OC_6H_3Bu^t_2$-2,6)$_2$(py)] **8** in solution. We have not been able to isolate **8** (*i.e.* free of additional pyridine), but its ^{1}H and ^{13}C-{^{1}H} NMR data support the proposed structure (Scheme 2) which is analogous to that of [Ti(NBu^t)($OC_6H_3Bu^t_2$-2,6)$_2$(py)] **4**.

Extended-Hückel molecular orbital calculations

At first sight the binuclear complex [Ti_2(μ-NBu^t)$_2$($OC_6H_3Me_2$-2,6)$_4$] **1** is formally an eighteen-valence-electron species. According to hybridisation theory, the near-linear Ti–O–R (R = aryl) angles and approximate planarity of the imido N atoms imply that the OR and NBu^t ligands are able to act as net five- and four-electron donors respectively. However, it is now recognised that such simple electron-counting approaches often fail in mono- and bi-nuclear complexes that contain a number of π-donor ligands.[21–30] The underlying reason is that the number of available metal d_π-acceptor orbitals (or symmetry-adapted linear combinations of d_π orbitals) *of the correct symmetry and energy* available for metal–ligand π bonding can be less than that required by all the available ligand p_π-donor orbitals.

The second interesting feature of the molecular structure of

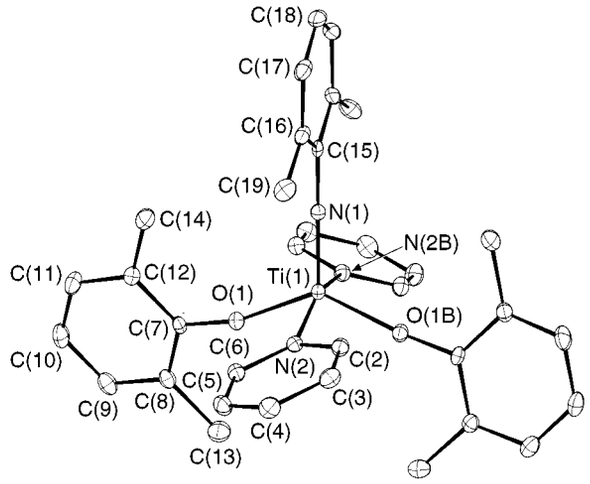

Fig. 2 A CAMERON[15] plot of [Ti($NC_6H_3Me_2$-2,6)($OC_6H_3Me_2$-2,6)$_2$(py)$_2$] **5**. Hydrogen atoms are omitted for clarity and the thermal ellipsoids are drawn at the 20% probability level. Atoms carrying the suffix B are related to their counterparts by the symmetry operator $-x, y, -z + \frac{1}{2}$

[Ti(μ-NBu^t)$_2$($OC_6H_3Me_2$-2,6)$_4$] is the displacement of the Bu^t imido substituents out of the Ti_2N_2 plane [N(1B) · · · N(1)–C(1) *ca.* 166°]. Taken by itself, this feature could be readily explained: steric factors could be invoked, for example. However, the apparent 'distortion' in **1** is in fact yet another example of a quite common feature in imido-bridged Group 4 complexes of the type [M_2(μ-$NR)_2L_4$]. We shall explore the origins of this feature in more detail below.

To probe more easily the electronic structure of [Ti_2(μ-NBu^t)$_2$($OC_6H_3Me_2$-2,6)$_4$] **1** we shall use the model complex [Ti_2(μ-$NH)_2$($OH)_4$] **A** with (initially) planar imido N atoms and linear Ti–O–H linkages. All other bond lengths and angles are taken from the real complex. In the D_{2h} symmetry of **A** the valence orbitals of the Ti_2, (μ-$NH)_2$ and $(OH)_4$ fragments can be analysed separately. The eight 4s and 4p orbitals of the Ti_2 fragment transform as $2a_g + b_{2g} + b_{3g} + 2b_{1u} + b_{2u} + b_{3u}$ and the ten 3d orbitals transform as $2a_g + a_u + b_{1g} + b_{2g} + b_{3g} + 2b_{1u} + b_{2u} + b_{3u}$. The σ-donor orbitals of the (μ-$NH)_2$ and $(OH)_4$ fragments transform as $a_g + b_{2g} + b_{1u} + b_{3u}$ and $a_g + b_{3g} + b_{1u} + b_{2u}$ respectively. The p_π donor orbitals of the (μ-$NH)_2$ and $(OH)_4$ fragments transform as $b_{1g} + b_{2u}$ and $a_g + a_u + b_{1g} + b_{2g} + b_{3g} + b_{1u} + b_{2u} + b_{3u}$ respectively under the D_{2h} symmetry of the complex. The Mulliken symbols for these irreducible representations assume the coordinate system shown in Fig. 4.

This elementary group-theoretical treatment immediately shows that two symmetry-adapted linear combinations (SALCs) (one a_g and one b_{1u}) of the Ti_2 fragment have no match with the σ + π donor SALCs of the {(μ-$NH)_2$($OH)_4$} ligand set. Similarly, two ligand-based SALCs (one b_{1g} and one b_{2u}) will end up as formally non-bonding lone pairs with respect to the Ti_2 fragment on symmetry arguments alone. Therefore it is already clear that the titanium centres in complex **1** can only ever achieve a maximum valence-electron count of sixteen.

It is important for our further analysis of the electronic structure of complex **1** to discuss next the nature of the two ligand-based p_π lone pairs (*i.e.* the non-bonding b_{1g} and b_{2u} SALCs) because these hold the key to understanding the distortion of the Bu^t groups from the Ti_2N_2 plane. Fig. 3 presents the necessary orbital sketches. Of the Ti_2 fragment SALCs there is only *one* b_{1g} d_π-acceptor SALC (at top left in Fig. 3). However, there are *two* ligand b_{1g} p_π-donor SALCs, one from the (μ-$NH)_2$ fragment (middle left) and one from the $(OH)_4$ fragment (bottom left). The Ti_2 fragment provides *two* b_{2u} SALCs, but one of these (mainly derived from two titanium 4p orbitals) will be used for Ti–O σ bonding. Therefore, as with the b_{1g} π interactions, two b_{2u} π-donor SALCs (middle right and bottom right

Table 3 Parameters used in the extended-Hückel molecular orbital calculations

Atom	Orbital	H_{ii}/eV	ζ_1
Ti*	3d	−12.48	4.231
	4s	−10.77	1.311
	4p	−5.92	1.088
N	2s	−26.00	1.950
	2p	−13.40	1.950
O	2s	−32.30	2.275
	2p	−14.80	2.275
H	1s	−13.60	1.300

* c_1 0.468, ζ_2 1.673, c_2 0.686.

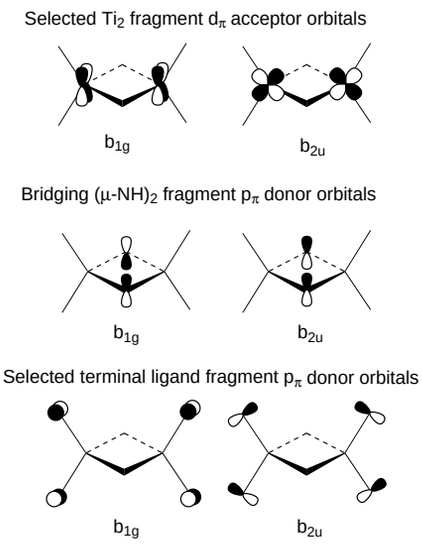

Fig. 3 The b_{1g} and b_{2u} Ti_2 d_π-acceptor, μ-NH p_π-donor and terminal ligand p_π-donor SALCs for $[Ti_2(\mu\text{-}NH)_2(OH)_4]$ **A** and $[Ti_2(\mu\text{-}NH)_2(NH_2)_4]$ **B**. For **B** the terminal ligand b_{2u} combination (bottom right) is used in NH σ bonding and so is not available for Ti–N π bonding. See the text for further details

in Fig. 3) compete for the one π-acceptor Ti_2 b_{1u}-symmetry d_π SALC (top right). The three π-bonding b_{1g} SALCs must give rise to a classic four-electron, three-orbital interaction[31] (one resultant molecular orbital, MO, will be metal–ligand π bonding, one will be effectively metal–ligand π-non-bonding and one will be metal–ligand π* antibonding). An analogous bonding situation will arise from the three b_{2u} SALCs. Although we can expect the metal–ligand non-bonding orbitals to be essentially ligand-based, we cannot *a priori* estimate the percentage nitrogen and oxygen orbital contribution to these orbitals (this will depend on the usual perturbation-theory arguments of overlap and energy differences). To help us address this aspect of our bonding analysis we have carried out full charge-iterative, extended-Hückel molecular orbital (EHMO) calculations[32] on both $[Ti_2(\mu\text{-}NH)_2(OH)_4]$ **A** and also on the hypothetical tetrakis(amido) complex $[Ti_2(\mu\text{-}NH)_2(NH_2)_4]$ **B**. The complex **B** is a model for the real compound $[Ti_2(\mu\text{-}NBu^t)_2(NMe_2)_4]$ which also has the Bu^t groups of the μ-imido ligands substantially bent out of the Ti_2N_2 plane [(μ-N)···(μ-N)–Bu^t *ca.* 161°].[18,19] The terminal $(NH_2)_4$ fragment in **B** has the same σ-donor characteristics as those of the terminal $(OH)_4$ fragment in **A** but only offers up four π-donor SALCs [as compared to eight from $(OH)_4$], simplifying the π-bonding framework somewhat (see below). The orbital parameters (energies and exponents) used in the EHMO calculations are listed in Table 3.

Fig. 4 presents the key results from the EHMO calculations as a simplified fragment-orbital interaction diagram for $[Ti_2(\mu\text{-}NH)_2(OH)_4]$ **A** and $[Ti_2(\mu\text{-}NH)_2(NH_2)_4]$ **B** in which we focus mainly on the b_{1g} and b_{2u} p_π–d_π interactions. At far left in Fig. 4 are shown the energies of the four N- and O-based b_{1g} and b_{2u} p_π-donor SALCs for **A**. At far right are the three analogous p_π-donor SALCs for **B**. Note that there is now only one b_{2u} ligand SALC available for p_π–d_π bonding in **B** since one (bottom right, Fig. 3) has been used in N–H σ bonding. At centre are shown the Ti_2 fragment b_{1g} and b_{2u} d_π acceptor orbitals together with what will become the (mainly) metal–ligand non-bonding a_g orbital identified in the initial group-theory analysis. The remaining energy levels (second from left and second from right respectively) in Fig. 4 result from allowing the Ti_2 and $\{(\mu\text{-}NH)_2(OH)_4\}$ and $\{(\mu\text{-}NH)_2(NH_2)_4\}$ fragments to interact.

The EHMO calculations wholly support the preliminary group-theoretical analysis. For species **A** the lowest unoccupied molecular orbital (LUMO) ($1a_g$) is effectively metal–ligand non-bonding and has 90% Ti atomic orbital character, while the metal–ligand non-bonding highest occupied molecular orbital (HOMO, $2b_{1g}$) and second highest occupied molecular orbital (SHOMO, $2b_{2u}$) have negligible metal character (12 and 13% Ti respectively). The HOMO and SHOMO are predominantly nitrogen-based with 62% N and 23% O and 60% N and 27% O character respectively. In other words, the μ-imido ligands in **A** are each acting as approximately three-electron donors due to the bridge/terminal p_π-donor conflict. For **B** a similar picture emerges with a metal-based LUMO ($1a_g$, 89% Ti) and a ligand-based HOMO ($2b_{1g}$, 44% bridging N and 56% terminal N character) that are both essentially metal–ligand non-bonding. However, in contrast to the situation for **A**, the depicted SHOMO ($1b_{2u}$) in **B** has full p_π–d_π bonding character because there is no longer a terminal ligand set b_{2u} p_π-donor SALC competing with the μ-imido b_{2u} p_π-donor SALC for the Ti_2 b_{2u} d_π-acceptor orbital. Therefore **B** has the μ-imido ligands acting as slightly better π donors to the dimetal centre. The remaining p_π–d_π levels shown for **A** and **B** represent the all-bonding ($1b_{1g}$ and $1b_{2u}$) and all-antibonding [$3b_{1g}$ and $3b_{2u}$ (**A**) or $2b_{2u}$ (**B**)] arrangements. However, it is the symmetries of the LUMO, HOMO and SHOMO (in **A** *and* **B**) that hold the key to understanding both the existence of the distortion of the Bu^t substituents out of the Ti_2N_2 plane and the *direction* of that distortion.

There are two potential out-of-plane distortions for the Bu^t substituents in $[Ti_2(\mu\text{-}NBu^t)_2(OC_6H_3Me_2\text{-}2,6)_4]$ **1** and $[Ti_2(\mu\text{-}NBu^t)_2(NMe_2)_4]$, namely centrosymmetric (one Bu^t group 'up' and one 'down', *i.e.* the one observed) or non-centrosymmetric (both Bu^t groups 'up' or both 'down'). The two possibilities are illustrated at the top of Fig. 5 for the model complex $[Ti_2(\mu\text{-}NH)_2(OH)_4]$ **A** which is viewed as a Newman projection along the Ti···Ti vector. The centrosymmetric distortion has B_{1g} symmetry in the D_{2h} point group and leads to a reduction in molecular symmetry to C_{2h}. The non-centrosymmetric mode has B_{2u} symmetry and lowers the molecule's point group to C_{2v}. Both distortions can be viewed as a manifestation of the second-order Jahn–Teller effect.[31]

In general, for a second-order Jahn–Teller distortion to occur at all the symmetry of the molecular distortion ($\Gamma_{distortion}$) must allow mixing between a filled and a vacant molecular orbital: thus for the HOMO and LUMO to mix, $\Gamma_{HOMO} \times \Gamma_{distortion} \times \Gamma_{LUMO}$ must contain the totally symmetric representation of the point group of the undistorted molecule. The effect is generally that the HOMO (or SHOMO) is stabilised and the LUMO (or next LUMO) is destabilised. Furthermore, for a second-order Jahn–Teller distortion to be substantial the interacting orbitals must lie close together in the non-distorted geometry.

Fig. 5 presents a partial Walsh diagram for the centrosymmetric (B_{1g}) and non-centrosymmetric (B_{2u}) distortions of $[Ti_2(\mu\text{-}NH)_2(OH)_4]$ **A**. The B_{1g} distortion allows the LUMO and HOMO of **A** to mix ($a_{1g} \times b_{1g} \times b_{1g} = a_{1g}$) thereby stabilising the HOMO, destabilising the LUMO (and SHOMO) and increasing the HOMO–LUMO gap. In contrast, the B_{2u} distortion coordinate mixes the LUMO and SHOMO ($a_{1g} \times b_{2u} \times b_{2u} = a_{1g}$) thereby stabilising the SHOMO, destabilising the LUMO (and HOMO) and also increasing the HOMO–LUMO

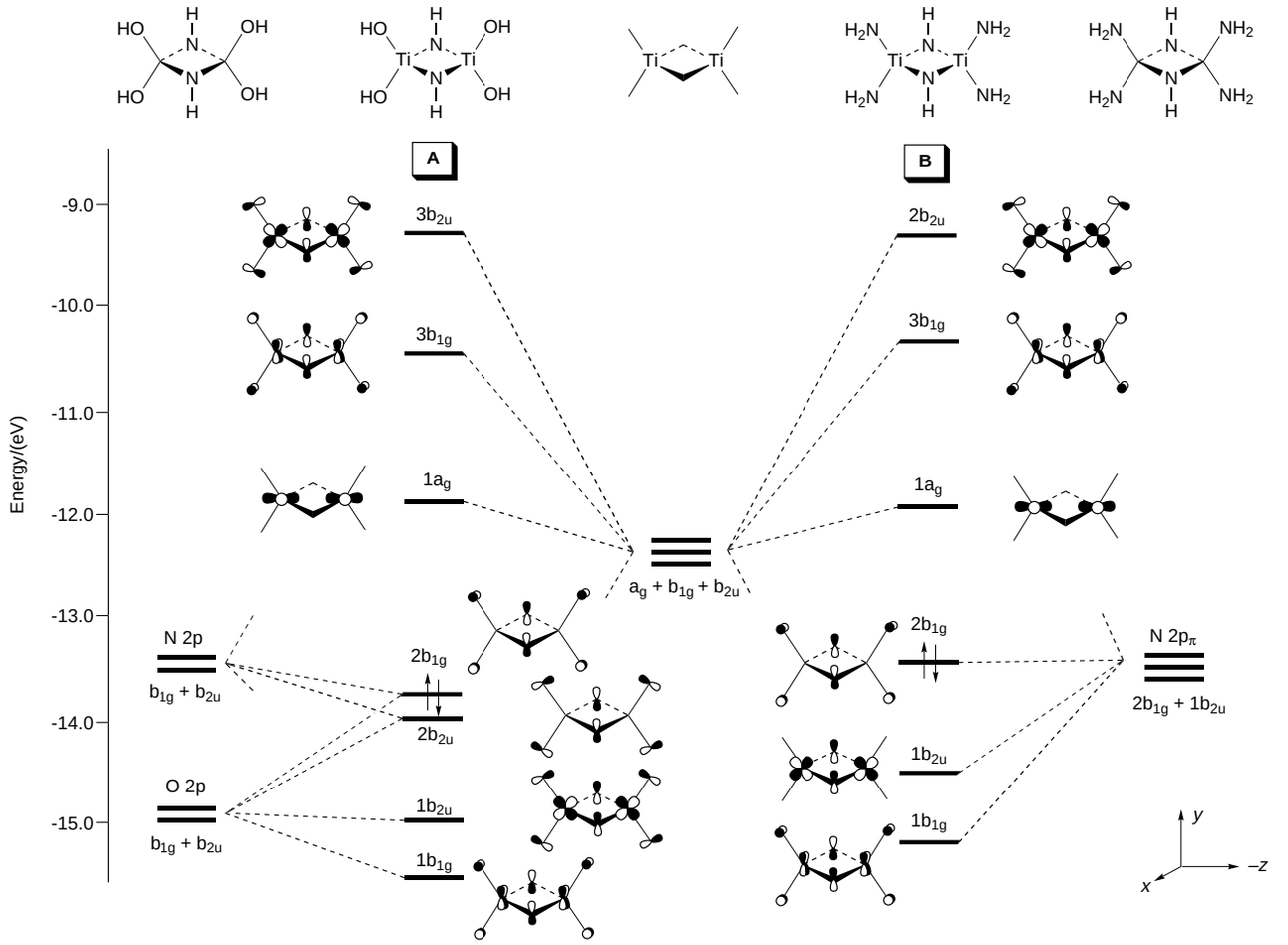

Fig. 4 Partial fragment molecular orbital interaction diagram for $[Ti_2(\mu\text{-}NH)_2(OH)_4]$ **A** and $[Ti_2(\mu\text{-}NH)_2(NH_2)_4]$ **B**. See the text for further details

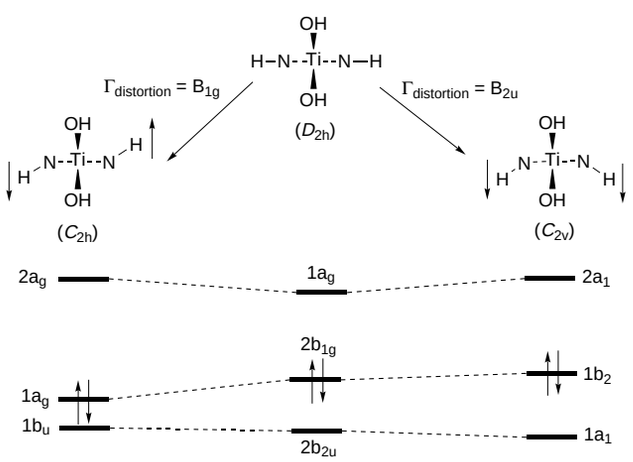

Fig. 5 Partial Walsh diagram for B_{1g} and B_{2u} molecular distortions of $[Ti_2(\mu\text{-}NH)_2(OH)_4]$ **A**. The molecules are shown as Newman projections viewed along the Ti···Ti vector. The orbital labels for C_{2h}- and C_{2v}-$[Ti_2(\mu\text{-}NH)_2(OH)_4]$ correspond to the usual choice of axes for these point groups. See the text for further details

gap. However, it is the centrosymmetric B_{1g} mode that is preferred. The computed second-order Jahn–Teller stabilisation energies for both distortions are quite modest, as would be expected since the calculated energy differences between the LUMO and HOMO/SHOMO in **A** are relatively large. Nonetheless, the calculations favour the B_{1g} mode over the B_{2u} alternative and this is easily rationalised from basic principles of molecular orbital theory.[31] First, the stabilisation of the HOMO for the B_{1g} distortion is twice that of the SHOMO for the B_{2u} mode (this is to be anticipated since the energy difference between the HOMO and LUMO in **A** is smaller by *ca.* 0.3 eV than that between the SHOMO and LUMO). Secondly, the increase in the HOMO–LUMO gap for the B_{1g} distortion mode is about twice that for the B_{2u} mode. This should also favour the B_{1g} distortion since it is generally found that the most stable of a selection of alternative molecular geometries is that possessing the largest HOMO–LUMO gap.

Having rationalised the preference of $[Ti_2(\mu\text{-}NBu^t)_2(OC_6H_3Me_2\text{-}2,6)_4]$ **1** for a centrosymmetric distortion of the NBu^t groups, it is easy to see why the tetrakis(dimethylamido) analogue $[Ti_2(\mu\text{-}NBu^t)_2(NMe_2)_4]$ also shows a centrosymmetric distortion. As the partial interaction diagram in Fig. 4 shows, the separation of the $1a_g$ (LUMO) and $2b_{1g}$ (HOMO) levels for the model complex $[Ti_2(\mu\text{-}NH)_2(NH_2)_4]$ **B** is smaller than that found for **A**. The $2b_{1g}$ level in **B** is less stable (due to having all nitrogen 2p contributions in **B** compared to two nitrogen 2p and four oxygen 2p contributions in **A**) and the $1a_g$ is slightly more stable than those for **A**. Furthermore, **B** does not possess a ligand-based, non-bonding SHOMO of b_{2u} symmetry. The $1b_{2u}$ level in **B** is metal–ligand d_π–p_π bonding and is considerably stabilised. Thus the B_{1g} distortion should therefore be considerably more favoured compared to the B_{2u} alternative, and also (since the HOMO–LUMO gap is smaller) should be slightly more significant than for **A**. Consistent with these expectations, the EHMO calculations found a larger stabilisation of the $2b_{1g}$ level along the B_{1g} distortion coordinate for complex **B** than for **A**. These theoretical results appear to be supported by the different extent of out-of-plane distortions in the real complexes $[Ti_2(\mu\text{-}NBu^t)_2(OC_6H_3Me_2\text{-}2,6)_4]$ [(μ-N)···(μ-N)–Bu^t *ca.* 166°] and $[Ti_2(\mu\text{-}NBu^t)_2(NMe_2)_4]$ [(μ-N)···(μ-N)–Bu^t *ca.* 161°].

In summary, therefore, our group-theoretical analysis and EHMO calculations have shown that the metal centres in $[Ti_2(\mu\text{-}NBu^t)_2(OC_6H_3Me_2\text{-}2,6)_4]$ **1** and $[Ti_2(\mu\text{-}NBu^t)_2(NMe_2)_4]$ can only ever achieve a maximum valence-electron count of

sixteen. They have also offered explanations for the origin and direction of the out-of-plane distortions of the μ-imido Bu^t substituents in both of these complexes.

Discussion

Synthesis

The synthetic routes (Schemes 1 and 2) to aryloxide-supported titanium imido complexes employed in these studies complement and extend those described previously by Rothwell and co-workers.[14,20] Our syntheses have generally given monomeric five-co-ordinate products and this arrangement appears therefore to be the most readily adopted. In addition, our routes also provide access to mono- and bi-nuclear four-co-ordinate complexes. The structures of aryloxide-supported titanium imido complexes depend critically on the identity of the aryloxide ligand *ortho* substituents and also on the imido nitrogen substituent. For example, $[Ti_2(\mu\text{-}NBu^t)_2(OC_6H_3Me_2\text{-}2,6)_4]$ **1** exists as a dimer (in the absence of an excess of free pyridine) whereas relatively minor O- or N-substituent changes give $[Ti(NBu^t)(OC_6H_3Pr^i_2\text{-}2,6)_2(py)_2]$ **3** or $[Ti(NC_6H_3Me_2\text{-}2,6)(OC_6H_3Me_2\text{-}2,6)_2(py)_2]$ **5** which both form monomeric complexes that are apparently stable to pyridine dissociation. Furthermore, in the absence of any *ortho* substituents {in the reaction of $[Ti(NBu^t)Cl_2(py)_3]$ with Li[OPh]} no tractable product is obtained.

We note that Bennett and Wolczanski[33] have recently described the highly reactive, transient three-co-ordinate species $[Ti(NSiBu^t_3)(OSiBu^t_3)_2]$ which may be trapped as a four-co-ordinate thf adduct analogous to $[Ti(NBu^t)(OC_6H_3Bu^t_2\text{-}2,6)_2(py)]$ **4**; in the absence of any suitable substrate it dimerises to form $[Ti_2(\mu\text{-}NSiBu^t_3)_2(OSiBu^t_3)_4]$, an analogue of $[Ti_2(\mu\text{-}NBu^t)_2(OC_6H_3Me_2\text{-}2,6)_4]$ **1**.

The solution behaviour of $[Ti(NC_6H_3Pr^i_2\text{-}2,6)(OC_6H_3Bu^t_2\text{-}2,6)_2(py)_2]$ **7** merits some discussion. The ^1H NMR spectra of this complex show two sets of pyridine resonances, one of which is exactly coincident with those of free pyridine under identical conditions. It is possible that the NMR data indicate a solution structure with two co-ordinated pyridine ligands in different environments (*e.g.* a trigonal-bipyramidal geometry with axial imido and pyridine ligands could account for the observed spectrum). However, we prefer to interpret the solution NMR data as being due to free pyridine and the four-co-ordinate species $[Ti(NC_6H_3Pr^i_2\text{-}2,6)(OC_6H_3Bu^t_2\text{-}2,6)_2(py)]$ **8**. The proposed structure for compound **8** is analogous to that unambiguously found for $[Ti(NBu^t)(OC_6H_3Bu^t_2\text{-}2,6)_2(py)]$ **4**. Additional support for this interpretation comes from our recently described series of *N*,*N*′-bis(trimethylsilyl)benzamidinate-supported complexes $[Ti(NR)\{PhC(NSiMe_3)_2\}Cl(py)_2]$ (R = Bu^t, $C_6H_3Me_2$-2,6 or $C_6H_3Pr^i_2$-2,6). These exist in the solid state as bis(pyridine) adducts but dissociate one of the pyridine ligands in solution.[11] Like **7**, these bis(pyridine) benzamidinate imido complexes do *not* release one of the pyridine ligands on extended heating under dynamic vacuum, again consistent with both pyridine ligands being co-ordinated in the solid state.

Crystal structures and bonding

The molecular structures of $[Ti_2(\mu\text{-}NBu^t)_2(OC_6H_3Me_2\text{-}2,6)_4]$ **1** (Fig. 1) and $[Ti(NC_6H_3Me_2\text{-}2,6)(OC_6H_3Me_2\text{-}2,6)_2(py)_2]$ **3** (Fig. 2) confirm and contrast the very different complexes obtained by making relatively minor changes to the aryloxide ligand *ortho*- and imido ligand nitrogen substituents. The compound **5** adopts pseudo-trigonal-bipyramidal structure with the pyridine ligands occupying the formally axial positions. The bond lengths and angles are comparable to those of $[Ti(NPh)(OC_6H_3Pr^i_2\text{-}2,6)_2L'_2]$ (L′ = 4-pyrrolidinopyridine).[14] A detailed account of transition-metal five-co-ordination has been reported previously by Rossi and Hoffmann;[34] an EHMO analysis of the π bonding in the congeneric zirconium amidoimido model complex $[Zr(NH)(NH_2)_2(NH_3)_2]$ has also been described and suggests that metal-imido π bonding dominates metal–amide π bonding.[14] A similar picture is expected to emerge for our aryloxide-supported imido complexes with metal–terminal imide π bonding dominating metal–aryloxide π bonding.

The molecular structure (Fig. 1) of the binuclear complex $[Ti_2(\mu\text{-}NBu^t)_2(OC_6H_3Me_2\text{-}2,6)_4]$ **1** is reminiscent of the tetrakis(dimethylamido) analogue $[Ti_2(\mu\text{-}NBu^t)_2(NMe_2)_4]$ first reported by Bradley and Torrible[17] and subsequently structurally characterised by Nugent and co-workers.[19] A search of the Cambridge Structural Database[16,17] showed that the structure of **1** is apparently also related to those of several other (pseudo-)four-co-ordinate, binuclear complexes of the general type $[Ti_2(\mu\text{-}NR)_2L_4]$ [R = Bu^t, aryl or organo-Si or -Sn; L_4 = (η-cyclopentadienyl, chloro)$_2$ or (amido, chloro)$_2$]. The basic geometric features of the central $\{Ti_2(\mu\text{-}NR)_2\}$ core of these complexes are very similar and most have the μ-N−R substituent bent out of the $Ti_2(\mu\text{-}N)_2$ plane [as defined by the (μ-N) ··· (μ-N)−R angle *ca*. 159 to 170° for all but one of seven examples].

Our group-theoretical and EHMO analysis of the out-of-plane Bu^t group distortion for complex **1** and Bradley's $[Ti_2(\mu\text{-}NBu^t)_2(NMe_2)_4]$ is consistent with an interpretation of this structural feature as a second-order Jahn–Teller effect (in these two complexes at least). Our results may also have a general relevance for other d^0 bimetallic μ-imido complexes. Furthermore, the extent of pyramidalisation of the μ-imido nitrogen atoms may give a qualitative indication of the relative π-donor ability of the terminal ligand set. While other analyses of the bonding in transition-metal binuclear μ-imido complexes have been described, they have not addressed this particular aspect of the electronic structure and molecular geometry.[19,28,29] In particular, the simple qualitative Hückel interpretation (*i.e.* treatment of the π-bonding framework alone) of Nugent and co-workers[19] for the model complex $[Ti_2(\mu\text{-}NH)_2(NH_2)_4]$ found a number of the basic features that our more detailed and extended analysis has revealed. These workers concluded that the μ-imido nitrogen atoms should posses 'a certain amount of "lone pair" character . . . and pyrimidalisation is not unreasonable'. We have shown this to be an insightful comment, not least because the pyramidal geometry of C_{3v}-NH_3 itself (having a 'full' lone pair) may quite validly be described as a second-order Jahn–Teller distortion of unstable, planar D_{3h}-NH_3.[31]

The overall effect of the second-order Jahn–Teller distortion of complex **1** and $[Ti_2(\mu\text{-}NBu^t)_2(NMe_2)_4]$ is to increase the donation of electron density from the ligand sets to the Ti_2 core. This shows up in the EHMO calculations as a reduction in net atomic positive charge for Ti, and of negative charge for N and O, along the distortion coordinate (Fig. 5) and occurs because the HOMO and LUMO can mix once the symmetry had been reduced to C_{2h}. Furthermore, it is quite likely that the extent of pyramidalisation of the μ-N atoms will correlate with the effectiveness of the π donation from the terminal atoms. It would be interesting if future studies of such systems find a relationship between the two quantities by, for example, varying the terminal N- or O-atom substituents.

Finally we note that the computed LUMO in $[Ti_2(\mu\text{-}NH)_2L_4]$ (L = OH or NH_2) is very well oriented for axial co-ordination of additional terminal ligands. Although **1** does not form a stable adduct with added pyridine, the binuclear, five-co-ordinate μ-oxo complex $[Ti_2(\mu\text{-}O)_2(OC_6H_3Pr^i_2\text{-}2,6)_4L'_2]$ has been crystallographically characterised.[35] It is possible that it is simply the lesser steric demands of the otherwise isoelectronic μ-oxo ligand (and/or the better the donor ability of L′) that permits the higher co-ordination number in this instance. More intriguing is the possibility that the pyramidalisation of the μ-N atoms itself is the root cause, since this has the effect of raising the LUMO in energy thus making it a less effective electron-pair-acceptor orbital.

Experimental

General methods and instrumentation

All manipulations were carried out under an atmosphere of argon or dinitrogen using standard Schlenk-line or dry-box techniques, respectively. All solvents and pyridine were pre-dried over activated molecular sieves and refluxed over the appropriate drying agent under an atmosphere of dinitrogen and collected by distillation. Deuteriochloroform was dried over freshly ground calcium hydride at r.t., distilled under vacuum and stored under N_2 in a Young's ampoule. The NMR samples were prepared in the dry-box in 5 mm Wilmad tubes equipped with a Young's Teflon valve. Proton and ^{13}C NMR spectra were recorded on either a Bruker DPX 300 or WM 250 spectrometer, referenced internally to residual protio-solvent (^1H) or solvent (^{13}C) resonances and are reported relative to tetramethylsilane (δ 0). Assignments were supported by distortionless enhancement by polarisation transfer (DEPT)-135 and DEPT-90, homo- and hetero-nuclear, one- and two-dimensional experiments as appropriate. Elemental analyses were carried out by the analytical laboratory of this department or by Canadian Microanalytical Service Ltd.

Starting materials

Phenols (Aldrich Chemical Co.) were used as received. The compounds $[Ti(NR)Cl_2(py)_3]$ (R = Bu^t, $C_6H_3Me_2$-2,6 or $C_6H_3Pr^i_2$-2,6) were prepared as previously described.[7] Lithium aryloxides were prepared by treating hexane solutions of the corresponding phenols with *n*-butyllithium in hexanes.

Preparations

$[Ti_2(\mu\text{-}NBu^t)_2(OC_6H_3Me_2\text{-}2,6)_4]$ 1. To a stirred solution of $[Ti(NBu^t)Cl_2(py)_3]$ (632 mg, 1.48 mmol) in thf (30 cm^3) at −25 °C was added a cold solution of $Li[OC_6H_3Me_2$-2,6] (379 mg, 2.96 mmol) in thf (25 cm^3). The mixture was allowed to warm to r.t. and stirred for 18 h to give a red solution. The volatiles were removed under reduced pressure and the sample was extracted into hexane (30 cm^3), filtered and the volatiles again removed under reduced pressure to leave a brown oil. The oil was extracted into pentane (25 cm^3) and after standing at r.t. for 5 min crystals appeared. The solution was decanted from the crystals and upon standing this produced even larger brown crystals after 1 h. The supernatant was decanted from the second crop and the crystals were washed with cold pentane (2 × 5 cm^3) and dried *in vacuo*. Total yield: 399 mg (37%). ^1H NMR ($CDCl_3$, 250 MHz): δ 7.01 (8 H, d, J = 7.3, *M*-H of $C_6H_3Me_2$), 6.79 (4 H, t, J = 7.4 Hz, *p*-H of $C_6H_3Me_2$), 2.42 (24 H, s, $C_6H_3Me_2$) and 1.24 (18 H, s, Bu^t). ^{13}C-{^1H} NMR ($CDCl_3$, 75.5 MHz): δ 162.7 (*ipso*-C of $C_6H_3Me_2$), 128.3 (*m*-C of $C_6H_3Me_2$), 126.8 (*o*-C of $C_6H_3Me_2$), 120.8 (*p*-C of $C_6H_3Me_2$), 73.3 (CMe_3), 33.1 (CMe_3) and 17.9 (2,6-$C_6H_3Me_2$) [Found (Calc. for $C_{40}H_{54}N_2O_4Ti_2$): C, 66.1 (66.5); H, 8.0 (7.5); N, 3.8 (3.9)%].

$[Ti(NBu^t)(OC_6H_3Me_2\text{-}2,6)_2(py)_2]$ 2. To a stirred solution of $[Ti(NBu^t)Cl_2(py)_3]$ (592 mg, 1.38 mmol) and pyridine (2.4 cm^3, 29.7 mmol) in thf (30 cm^3) at r.t. was added a solution of $Li[OC_6H_3Me_2$-2,6] (358 mg, 2.77 mmol) in thf (25 cm^3). The mixture was stirred for 18 h to give a yellow solution and the volatiles were removed under reduced pressure. The residues were extracted into hexane (30 cm^3) containing pyridine (2.5 cm^3) and the solution was filtered. Attempted low-temperature crystallisation of complex **2** from reduced volumes of these hexane–pyridine solutions was unsuccessful. Thus the volatiles were removed under reduced pressure to leave a yellow-orange oil that was shown by NMR spectroscopy to contain **2** and some free pyridine. The amount of free pyridine varies between preparations. ^1H NMR ($CDCl_3$, 250 MHz): δ 8.85 (asymmetric br s, overlapping free and co-ordinated *o*-H of NC_5H_5), 7.73 (t, J = 7.7, overlapping free and co-ordinated *p*-H of NC_5H_5), 7.29 (apparent t, apparent J = 7.3 Hz, overlapping free and co-ordinated *m*-H of NC_5H_5), 6.96 (4 H, d, J = 7.3, *m*-H of $C_6H_3Me_2$), 6.58 (2 H, t, J = 7.3 Hz, *p*-H of $C_6H_3Me_2$), 2.20 (12 H, s, $C_6H_3Me_2$) and 0.89 (9 H, s, Bu^t). ^{13}C-{^1H} NMR ($CDCl_3$, 75.5 MHz): δ 161.6 (*ipso*-C of $C_6H_3Me_2$), 149.9 (overlapping free and co-ordinated *o*-C of NC_5H_5), 135.9 (overlapping free and co-ordinated *p*-C of NC_5H_5), 127.7 (*m*-C of $C_6H_3Me_2$), 126.6 (*o*-C of $C_6H_3Me_2$), 123.8 (overlapping free and co-ordinated *m*-C of NC_5H_5), 116.5 (*p*-C of $C_6H_3Me_2$), 68.7 (CMe_3), 31.7 (CMe_3) and 17.6 ($C_6H_3Me_2$). Satisfactory elemental analysis was not obtained.

$[Ti(NBu^t)(OC_6H_3Pr^i_2\text{-}2,6)_2(py)_2]$ 3. To a stirred solution of $[Ti(NBu^t)Cl_2(py)_3]$ (591 mg, 1.38 mmol) in thf (30 cm^3) at −40 °C was added a cold solution of $Li[OC_6H_3Pr^i_2$-2,6] (509 mg, 2.77 mmol) in thf (30 cm^3). The solution was allowed to warm to r.t. and after 15 h the volatiles were removed under reduced pressure. The yellow solid was extracted into diethyl ether (20 cm^3), filtered and placed at −25 °C to yield yellow crystals. Yield: 515 mg (59%). ^1H NMR ($CDCl_3$, 250 MHz); δ 8.90 (4 H, d, J = 4.8, *o*-H of NC_5H_5), 7.74 (2 H, t, J = 7.7, *p*-H of NC_5H_5), 7.30 (4 H, apparent t, apparent J = 6.8, *m*-H of NC_5H_5), 7.06 (4 H, d, J = 7.5, *m*-C of $C_6H_3Pr^i_2$), 6.77 (2 H, t, J = 7.5, *p*-C of $C_6H_3Pr^i_2$), 4.00 (4 H, spt, J = 6.9, $CHMe_2$), 1.05 (24 H, d, J = 6.9 Hz, $CHMe_2$) and 0.95 (9 H, s, Bu^t). ^{13}C-{^1H} NMR ($CDCl_3$, 75.5 MHz): δ 158.1 (*ipso*-C of $C_6H_3Pr^i_2$), 150.3 (*o*-C of NC_5H_5), 137.7 (*p*-C of NC_5H_5), 137.2 (*o*-C of $C_6H_3Pr^i_2$), 124.0 (*m*-C of $C_6H_3Pr^i_2$), 122.8 (*m*-C of NC_5H_5), 117.2 (*p*-C of $C_6H_3Pr^i_2$), 68.8 (CMe_3), 31.7 (CMe_3), 25.4 ($CHMe_2$) and 23.9 ($CHMe_2$) [Found (Calc. $C_{38}H_{53}N_3O_2Ti$): C, 72.2 (72.3); H, 8.5 (8.5); N, 6.4 (6.7)%].

$[Ti(NBu^t)(OC_6H_3Bu^t_2\text{-}2,6)_2(py)]$ 4. To a stirred solution of $[Ti(NBu^t)Cl_2(py)_3]$ (615 mg, 1.44 mmol) in thf (25 cm^3) at −50 °C was added a cold solution of $Li[OC_6H_3Bu^t_2$-2,6] (611 mg, 2.88 mmol) in thf (25 cm^3). The solution was allowed to warm to r.t. and after 16 h the volatiles were removed under reduced pressure. The pale orange solid was extracted into dichloromethane (25 cm^3). Careful layering of this solution with pentane (15 cm^3) and recrystallisation at −25 °C yielded orange crystals which were washed with cold pentane (2 × 5 cm^3) and dried *in vacuo*. Yield: 707 mg (81%). ^1H NMR ($CDCl_3$, 250 MHz): δ 9.21 (2 H, d, J = 4.9, *o*-H of NC_5H_5), 8.03 (1 H, t, J = 7.7, *p*-H of NC_5H_5), 7.58 (2 H, apparent t, apparent J = 7.6, *m*-H of NC_5H_5), 7.25 (4 H, d, J = 7.8, *m*-H of $C_6H_3Bu^t_2$), 6.76 (2 H, t, J = 7.7, *p*-H of $C_6H_3Bu^t_2$), 1.50 (36 H, s, $C_6H_3Bu^t_2$) and 0.94 (9 H, NBu^t). ^{13}C-{^1H} NMR ($CDCl_3$, 62.9 MHz): δ 164.3 (*ipso*-C of $C_6H_3Bu^t_2$), 151.7 (*o*-C of NC_5H_5), 140.3 (*p*-C of NC_5H_5), 138.5 (*o*-C of $C_6H_3Bu^t_2$), 125.0 (*m*-C of $C_6H_3Bu^t_2$), 124.7 (*m*-C of NC_5H_5), 117.7 (*p*-C of $C_6H_3Bu^t_2$), 72.1 ($NCMe_3$), 35.4 [$C_6H_3(CMe_3)_2$], 31.8 [$C_6H_3(CMe_3)_2$] and 31.6 ($NCMe_3$) [Found (Calc. for $C_{37}H_{56}N_2O_2Ti$): C, 72.9 (73.0); H, 9.5 (9.3); N, 4.4 (4.6)%].

$[Ti(NC_6H_3Me_2\text{-}2,6)(OC_6H_3Me_2\text{-}2,6)_2(py)_2]$ 5. To a stirred solution of $[Ti(NC_6H_3Me_2$-2,6)$Cl_2(py)_3]$ (883 mg, 1.84 mmol) in thf (20 cm^3) at −50 °C was added a cold solution of $Li[OC_6H_3Me_2$-2,6] (472 mg, 3.68 mmol) in thf (20 cm^3). The resulting red solution was allowed to warm to r.t. and stirred for 15 h. The volatiles were removed under reduced pressure and the solid was extracted into hexane (2 × 25 cm^3). Recrystallisation from hexane at −25 °C afforded red-brown crystals which were washed with cold diethyl ether (2 × 5 cm^3) was dried *in vacuo*. Yield: 649 mg (62%). ^1H NMR ($CDCl_3$, 300 MHz): δ 8.90 (4 H, br d, J = 3.6, *o*-H of NC_5H_5), 7.77 (2 H, t, J = 7.4, *p*-H of NC_5H_5), 7.31 (4 H, apparent t, apparent J = 6.8, *m*-H of NC_5H_5), 6.99 (4 H, d, J = 7.4, *m*-H of $OC_6H_3Me_2$), 6.69 (4 H, overlapping 2 × m, *m*-H of $NC_6H_3Me_2$ and *p*-H of $C_6H_3Me_2$), 6.43 (1 H, t, J = 7.4 Hz, *p*-H of $NC_6H_3Me_2$), 2.24 (12 H, s, $OC_6H_3Me_2$) and 1.85 (6 H, s, $NC_6H_3Me_2$). ^{13}C-{^1H} NMR

Table 4 X-Ray data collection and processing parameters for $[Ti_2(\mu\text{-}NBu^t)_2(OC_6H_3Me_2\text{-}2,6)_4]$ **1** and $[Ti(NC_6H_3Me_2\text{-}2,6)(OC_6H_3Me_2\text{-}2,6)_2(py)_2]$ **5***

	1	**5**
Empirical formula	$C_{40}H_{54}N_2O_4Ti_2$	$C_{34}H_{37}N_3O_2Ti$
M	722.68	567.57
Crystal size/mm	0.09 × 0.06 × 0.05	0.59 × 0.58 × 0.12
Space group	$P2_1/c$	$C2/c$
a/Å	10.076(4)	13.842(6)
b/Å	13.238(6)	11.923(4)
c/Å	14.836(2)	19.914(9)
β/°	97.02(2)	106.04(3)
U/Å^3	1964	3159
Z	2	4
D_c/g cm^{-3}	1.22	1.19
μ/mm^{-1}	0.44	0.30
F(000)	768	1200
Index ranges	$-10 \leqslant h \leqslant 8$, $-14 \leqslant k \leqslant 9$, $-17 \leqslant l \leqslant 15$	$-14 \leqslant h \leqslant 14$, $-10 \leqslant k \leqslant 12$, $-21 \leqslant l \leqslant 15$
θ Range/°	2.1–25.1	2.7–25.0
Reflections collected	4539	4033
Independent reflections, R_{int}	2647, 0.062	2106, 0.072
No. observations [$I > 2\sigma(I)$]	2224	1662
Absorption correction	None applied	ψ Scans
maximum, minimum transmission	—	0.875, 0.697
No. variables	218	186
Weighting scheme	Chebychev polynominal[36]	$[\sigma^2(F_o^2) + (0.021P)^2 + 6.01P]^{-1}$ where $P = \frac{1}{3}[\max(F_o^2, 0) + 2F_c^2]$
Largest difference peak and hole/e Å^{-3}	0.70, −0.54	0.23, −0.31
Final R1, $wR2$ indices [$F > 4\sigma(F)$]	0.053, 0.059	0.048, 0.097
(all data)	0.0580, 0.0639	0.071, 0.112
Goodness of fit on F^2	1.132	1.153

* Details in common: 150 K; λ(Mo-Kα) 0.710 73 Å; crystal colour red; monoclinic; full-matrix refinement on F_o^2; no restraints; $R1 = \Sigma||F_o| - |F_c||/\Sigma|F_o|$; $wR2 = [\Sigma w(F_o^2 - F_c^2)^2/\Sigma w(F_o^2)^2]^{\frac{1}{2}}$; goodness of fit = $[\Sigma w(F_o^2 - F_c^2)^2/(N_{obs} - N_{param})]^{\frac{1}{2}}$ based on all data.

($CDCl_3$, 75.5 MHz): δ 161.7, 159.3 (*ipso*-C of $NC_6H_3Me_2$ and *ipso*-C of $OC_6H_3Me_2$), 150.2 (*o*-C of NC_5H_5), 137.9 (*p*-C of NC_5H_5), 129.7 (*o*-C of $NC_6H_3Me_2$), 128.1 (*m*-C of $OC_6H_3Me_2$), 127.0 (*m*-C of $NC_6H_3Me_2$), 126.8 (*o*-C of $OC_6H_3Me_2$), 124.2 (*m*-C of NC_5H_5), 117.8 (overlapping *p*-C of $NC_6H_3Me_2$ and *p*-C of $OC_6H_3Me_2$), 18.8 ($NC_6H_3\mathit{Me}_2$) and 17.6 ($OC_6H_3\mathit{Me}_2$) [Found (Calc. for $C_{34}H_{37}N_3O_2Ti$): C, 71.9 (72.0); H, 6.6 (6.6); N, 7.4 (7.4)%].

$[Ti(NC_6H_3Pr^i_2\text{-}2,6)(OC_6H_3Me_2\text{-}2,6)_2(py)_2]$ 6. To a stirred solution of $[Ti(NC_6H_3Pr^i_2\text{-}2,6)Cl_2(py)_3]$ (447 mg, 0.842 mmol) in thf (20 cm^3) at −50 °C was added a cold solution of $Li[OC_6H_3Me_2\text{-}2,6]$ (216 mg, 1.68 mmol) in thf (20 cm^3). The red solution was allowed to warm to r.t. and stirred for 14 h. The volatiles were removed under reduced pressure and the red solid was extracted into hexane (2 × 40 cm^3) and filtered. The orange solution was cooled (−25 °C) yielding red-brown crystals. Yield: 189 mg (36%). ^{1}H NMR ($CDCl_3$, 300 MHz): δ 8.90 (4 H, d, J = 3.6, *o*-H of NC_5H_5), 7.79 (2 H, t, J = 7.6, *p*-H of NC_5H_5), 7.33 (4 H, t, J = 6.9, *m*-H of NC_5H_5), 7.00 (4 H, d, J = 7.5, *m*-H of $C_6\mathit{H}_3Me_2$), 6.77 (2 H, d, J = 7.5, *m*-H of $C_6\mathit{H}_3Pr^i_2$), 6.68 (2 H, t, J = 7.5, *p*-H of $C_6\mathit{H}_3Me_2$), 6.59 (1 H, t, J = 7.5, *p*-H of $C_6\mathit{H}_3Pr^i_2$), 3.57 (2 H, spt, J = 6.9, C$\mathit{H}Me_2$), 2.20 (12 H, s, $C_6H_3\mathit{Me}_2$) and 0.73 (12 H, d, J = 6.9 Hz, CHMe_2). ^{13}C-{^{1}H} NMR ($CDCl_3$, 75.5 MHz): δ 161.6, 156.5 (*ipso*-C of $\mathit{C}_6H_3Pr^i_2$ and of $\mathit{C}_6H_3Me_2$), 150.3 (*o*-C of NC_5H_5), 141.0 (*o*-C of $\mathit{C}_6H_3Pr^i_2$), 138.0 (*p*-C of NC_5H_5), 128.1 (*m*-C of $\mathit{C}_6H_3Me_2$), 126.8 (*o*-C of $\mathit{C}_6H_3Me_2$), 124.4 (*m*-C of NC_5H_5), 121.8 (*m*-C of $\mathit{C}_6H_3Pr^i_2$), 118.5 (*p*-C of $\mathit{C}_6H_3Pr^i_2$), 117.8 (*p*-C of $\mathit{C}_6H_3Me_2$), 27.2 ($\mathit{C}HMe_2$), 23.8 (CHMe_2) and 17.6 ($C_6H_3\mathit{Me}_2$) [Found (Calc. for $C_{38}H_{45}N_3O_2Ti$): C, 74.1 (73.2); H, 7.9 (7.3); N, 6.7 (6.7)%].

$[Ti(NC_6H_3Pr^i_2\text{-}2,6)(OC_6H_3Bu^t_2\text{-}2,6)_2(py)_2]$ 7/$[Ti(NC_6H_3Pr^i_2\text{-}2,6)(OC_6H_3Bu^t_2\text{-}2,6)_2(py)]$ 8. To a stirred solution of $[Ti(NC_6H_3Pr^i_2\text{-}2,6)Cl_2(py)_3]$ (417 mg, 0.785 mmol) in thf (20 cm^3) at −50 °C was added a cold solution of $Li[OC_6H_3Bu^t_2\text{-}2,6]$ (335 mg, 1.57 mmol) in thf (20 cm^3). The solution was allowed to warm to r.t. and stirred for 16 h. The volatiles were removed under reduced pressure and the brown solid was extracted into diethyl ether (30 cm^3). The solution was concentrated to 20 cm^3 and recrystallisation at −25 °C afforded brown crystals which were washed with cold diethyl ether (2 × 5 cm^3) and dried *in vacuo*. Yield: 198 mg (32%). Compound **7** gives rise to the mono-pyridine adduct **8** and free pyridine in solution. The following NMR data are assigned accordingly. ^{1}H NMR ($CDCl_3$, 300 MHz): δ 9.32 (2 H, d, J = 6.4, *o*-H of NC_5H_5), 8.67 (2 H, br s, free *o*-H of NC_5H_5), 8.11 (1 H, t, J = 6.9, *p*-H of NC_5H_5), 7.70 (2 H, m, free *p*-H of NC_5H_5), 7.66 (1 H, apparent t, apparent J = 6.5, *m*-H of NC_5H_5), 7.32 (2 H, apparent t, apparent J = 6.9, free *m*-H of NC_5H_5), 7.23 (4 H, d, J = 7.8, *m*-H of $C_6\mathit{H}_3Bu^t_2$), 6.81 (2 H, d, J = 7.7, *p*-H of $C_6\mathit{H}_3Bu^t_2$), 6.78 (2 H, t, J = 6.0, *p*-H of $C_6\mathit{H}_3Pr^i_2$), 6.67 (1 H, t, J = 6.6, *p*-H of $C_6\mathit{H}_3Pr^i_2$), 3.59 (2 H, spt, J = 6.8, C$\mathit{H}Me_2$), 2.20 (36 H, s, $C_6H_3\mathit{Bu}^t_2$) and 0.78 (12 H, d, J = 6.8 Hz, CHMe_2). ^{13}C-{^{1}H} NMR ($CDCl_3$, 75.5 MHz): δ 164.8, 157.1 (*ipso*-C of $\mathit{C}_6H_3Pr^i_2$ and of $\mathit{C}_6H_3Bu^t_2$), 150.8 (*o*-C of NC_5H_5), 149.8 (free *o*-C of NC_5H_5), 142.2 (*o*-C of $\mathit{C}_6H_3Pr^i_2$), 140.6 (*p*-C of NC_5H_5), 138.3 (*o*-C of $\mathit{C}_6H_3Bu^t_2$), 135.8 (free *p*-C of NC_5H_5), 125.1 (overlapping *m*-C of NC_5H_5 and of $\mathit{C}_6H_3Bu^t_2$), 123.6 (free *m*-C of NC_5H_5), 121.7 (*m*-C of $\mathit{C}_6H_3Pr^i_2$), 120.7 (*p*-C of $\mathit{C}_6H_3Pr^i_2$), 118.7 (*p*-C of $\mathit{C}_6H_3Bu^t_2$), 35.3 [$C_6H_3(\mathit{C}Me_3)_2$], 31.7 [$C_6H_3(C\mathit{Me}_3)_2$], 27.4 ($\mathit{C}HMe_2$) and 23.9 (CHMe_2) [Found (Calc. for $C_{50}H_{69}N_3O_2Ti$): C, 73.1 (75.8); H, 9.0 (8.8); N, 4.6 (5.3)%]. The low values for C and N may indicate partial loss of pyridine in the precombustion phase of the analysis.

Crystallography

X-Ray data collection and processing parameters are given in Table 4. Crystallographic and data collection measurements for complex **1** were made using a Delft FAST TV area detector diffractometer according to previously described procedures.[37] For **5** crystals were mounted on a glass fibre with RS3000 oil and transferred to the goniometer head of a Stoë Stadi-4 four-

circle diffractometer equipped with an Oxford Cryosystems low-temperature device.[38]

Equivalent reflections were merged and systematically absent reflections were rejected. For the plate-shaped crystal of complex **5** an absorption correction based on ψ scans was applied. The structures were solved by direct methods using SIR 92[39] (for **1**) and heavy-atom methods. Subsequent Fourier-difference syntheses revealed the positions of all non-hydrogen atoms which were refined anisotropically. Molecules of **1** lie across crystallographic inversion centres. Molecules of **5** lie on crystallographic two-fold rotation axes passing through atoms Ti(1), N(1), C(15) and C(18). Hydrogen atoms were placed in calculated positions and refined using a 'riding' model. For both complexes weighting schemes were applied; examination of the refined secondary extinction parameter and comparison of $|F_o|$ and $|F_c|$ for the strongest reflections suggested that no extinction correction was required.

Crystallographic calculations for complex **1** were performed using SIR 92[39] and CRYSTALS-PC[40] (for **1**) and SHELXL 96[41] (for **5**).

CCDC reference number 186/616.

Extended-Hückel molecular orbital calculations

The geometries of the model complexes $[Ti_2(\mu\text{-}NH)_2(OH)_4]$ **A** and $[Ti_2(\mu\text{-}NH)_2(NH_2)_4]$ **B** were based on the crystal structures of the real complexes $[Ti_2(\mu\text{-}NBu^t)_2(OC_6H_3Me_2\text{-}2,6)_4]$ **1** and $[Ti_2(\mu\text{-}NBu^t)_2(NMe_2)_4]$[19] respectively and idealised to D_{2h} symmetry. The 4s, 4p and 3d orbital H_{ii} values for Ti (Table 3) were obtained from charge-iterative calculations on $[Ti_2(\mu\text{-}NH)_2(OH)_4]$. The titanium valence-orbital exponents were taken from the work of Fitzpatrick and Murphy.[42] The orbital energies and exponents for C, N, O and H are the standard ones.[43] Charge-iterative calculations were carried out using the TRIBBLE suite of programs held on the Oxford University Computer Service VAX cluster. All other EHMO calculations were performed using the CACAO package.[44]

Acknowledgements

This work was in part supported by grants (to P. M.) from the EPSRC, Leverhulme Trust and Royal Society. We thank the University of Nottingham for a Demonstratorship (to P. E. C.), Professor M. B. Hursthouse and the EPSRC Crystallography Service for the X-ray data for complex **1**, the EPSRC for the provision of a diffractometer, Ms. J. M. Vere and Mr. M. D. Walker for assisting with the preparation of some of the compounds and Dr. W.-S. Li for help with X-ray data collection. We also acknowledge the use of the EPSRC's Chemical Database Service at CCLRC Daresbury Laboratory.

References

1 W. A. Nugent and B. L. Haymore, *Coord. Chem. Rev.*, 1980, **31**, 123.
2 W. A. Nugent and J. M. Mayer, *Metal–Ligand Multiple Bonds*, Wiley-Interscience, New York, 1988.
3 D. E. Wigley, *Prog. Inorg. Chem.*, 1994, **42**, 239.
4 H. W. Roesky, H. Voelker, M. Witt and M. Noltemeyer, *Angew. Chem., Int. Ed. Engl.*, 1990, **29**, 669.
5 J. E. Hill, R. D. Profilet, P. E. Fanwick and I. P. Rothwell, *Angew. Chem., Int. Ed. Engl.*, 1990, **29**, 664.
6 S. C. Dunn, A. S. Batsanov and P. Mountford, *J. Chem. Soc., Chem. Commun.*, 1994, 2007.
7 A. J. Blake, P. E. Collier, S. C. Dunn, W.-S. Li, P. Mountford and O. V. Shishkin, *J. Chem. Soc., Dalton Trans.*, 1997, 1549.
8 S. C. Dunn, P. Mountford and D. A. Robson, *J. Chem. Soc., Dalton Trans.*, 1997, 293.
9 P. Mountford, *J. Organomet. Chem.*, 1997, **528**, 15.
10 S. C. Dunn, P. Mountford and O. V. Shishkin, *Inorg. Chem.*, 1996, **35**, 1006.
11 P. J. Stewart, A. J. Blake and P. Mountford, *Inorg. Chem.*, 1997, in the press.
12 A. J. Blake, P. Mountford, G. I. Nikonov and D. Swallow, *Chem. Commun.*, 1996, 1835.
13 P. Mountford and D. Swallow, *J. Chem. Soc., Chem. Commun.*, 1995, 2357.
14 C. H. Zambrano, R. D. Profilet, J. E. Hill, P. E. Fanwick and I. P. Rothwell, *Polyhedron*, 1993, **12**, 689.
15 D. J. Watkin, C. K. Prout and L. J. Pearce, CAMERON, Chemical Crystallography Laboratory, University of Oxford, 1996.
16 F. H. Allen and O. Kennard, *Chem. Des. Autom. News*, 1993, **8**, 1 and 31.
17 D. A. Fletcher, R. F. McMeeking and D. Parkin, *J. Chem. Inf. Comput. Sci.*, 1996, **36**, 746.
18 D. C. Bradley and E. G. Torrible, *Can. J. Chem.*, 1963, **41**, 134.
19 D. L. Thorn, W. A. Nugent and R. L. Harlow, *J. Am. Chem. Soc.*, 1981, **103**, 357.
20 J. E. Hill, P. E. Fanwick and I. P. Rothwell, *Inorg. Chem.*, 1991, **30**, 1143.
21 A. J. Bridgeman, L. Davis, S. J. Dixon, J. C. Green and I. N. Wright, *J. Chem. Soc., Dalton Trans.*, 1995, 1023.
22 J. C. Green, M. L. H. Green, J. T. James, P. C. Konidaris, G. H. Maunder and P. Mountford, *J. Chem. Soc., Chem. Commun.*, 1992, 1361.
23 N. D. Silavwe, M. R. M. Bruce, C. E. Philbin and D. R. Tyler, *Inorg. Chem.*, 1988, **27**, 4669.
24 G. Parkin, A. van Asselt, D. J. Leahy, L. Whinnery, N. G. Hua, R. W. Quan, L. M. Henling, W. P. Schaefer, B. D. Santarsiero and J. E. Bercaw, *Inorg. Chem.*, 1992, **31**, 82.
25 J. H. Osborne and W. C. Trogler, *Inorg. Chem.*, 1985, **24**, 3098.
26 M. H. Schofield, T. P. Kee, J. T. Anhaus, R. R. Schrock, K. H. Johnson and W. M. Davis, *Inorg. Chem.*, 1991, **30**, 3595.
27 M. T. Benson, J. C. Bryan, A. K. Burrell and T. R. Cundari, *Inorg. Chem.*, 1995, **34**, 2348.
28 A. K. Burrell. D. L. Clark, P. L. Gordon, A. P. Sattelberger and J. C. Bryan, *J. Am. Chem. Soc.*, 1994, **116**, 3813.
29 M. L. H. Green, G. Hogarth, P. C. Konidaris and P. Mountford, *J. Chem. Soc., Dalton Trans.*, 1990, 3781.
30 Z. Lin and M. B. Hall, *Coord. Chem. Rev.*, 1993. **123**, 149.
31 T. A. Albright, J. K. Burdett and M.-H. Whangbo, *Orbital Interactions in Chemistry*, Wiley-Interscience, New York, 1985.
32 R. Hoffmann and W. N. Lipscomb, *J. Chem. Phys.*, 1962, **36**, 2179.
33 J. L. Bennett and P. T. Wolczanski, *J. Am. Chem. Soc.*, 1994, **116**, 2179.
34 A. R. Rossi and R. Hoffmann, *Inorg. Chem.*, 1975, **14**, 365.
35 J. E. Hill, P. E. Fanwick and I. P. Rothwell, *Acta Crystallogr., Sect. C*, 1991, **47**, 541.
36 J. R. Carruthers and D. J. Watkin, *Acta Crystallogr., Sect. A*, 1979, **35**, 698.
37 J. A. Darr, S. R. Drake, M. B. Hursthouse and K. M. A. Malik, *Inorg. Chem.*, 1993, **32**, 5704.
38 J. Cosier and A. M. Glazer, *J. Appl. Crystallogr.*, 1986, **19**, 105.
39 A. Altomare, G. Cascarano, G. Giacovazzo, A. Guagliardi, M. C. Burla, G. Polidori and M. Carnalli, *J. Appl. Crystallogr.*, 1994, **27**, 435.
40 D. J. Watkin, C. K. Prout, J. R. Carruthers and P. W. Betteridge, *CRYSTALS Issue 10*, Chemical Crystallography Laboratory, University of Oxford, 1996.
41 G. M. Sheldrick, SHELXL 96, Institut für Anorganische Chemie der Universität Göttingen, 1996.
42 N. J. Fitzpatrick and G. H. Murphy, *Inorg. Chim. Acta*, 1986, **111**, 139.
43 R. Hoffmann, *J. Chem. Phys.*, 1963, **39**, 1397.
44 C. Mealli and D. M. Proserpio, *J. Chem. Educ.*, 1990, **67**, 3399.

Received 13*th May* 1997; *Paper* 7/03309E